



Observation of Vortex Dipoles in an Oblate Bose-Einstein Condensate

T. W. Neely,¹ E. C. Samson,¹ A. S. Bradley,² M. J. Davis,³ and B. P. Anderson^{1,4}

¹*College of Optical Sciences, University of Arizona, Tucson, Arizona 85721, USA*

²*Jack Dodd Centre for Quantum Technology, Department of Physics, University of Otago, Post Office Box 56, Dunedin, New Zealand*

³*The University of Queensland, School of Mathematics and Physics, ARC Centre of Excellence for Quantum-Atom Optics, Queensland 4072, Australia*

⁴*Department of Physics, University of Arizona, Tucson, Arizona 85721, USA*

(Received 17 December 2009; published 19 April 2010)

We report experimental observations and numerical simulations of the formation, dynamics, and lifetimes of single and multiply charged quantized vortex dipoles in highly oblate dilute-gas Bose-Einstein condensates (BECs). We nucleate pairs of vortices of opposite charge (vortex dipoles) by forcing superfluid flow around a repulsive Gaussian obstacle within the BEC. By controlling the flow velocity we determine the critical velocity for the nucleation of a single vortex dipole, with excellent agreement between experimental and numerical results. We present measurements of vortex dipole dynamics, finding that the vortex cores of opposite charge can exist for many seconds and that annihilation is inhibited in our trap geometry. For sufficiently rapid flow velocities, clusters of like-charge vortices aggregate into long-lived multiply charged dipolar flow structures.

DOI: [10.1103/PhysRevLett.104.160401](https://doi.org/10.1103/PhysRevLett.104.160401)

PACS numbers: 03.75.Kk, 03.75.Lm, 67.85.De

A vortex dipole in a classical or quantum fluid consists of a pair of vortices of opposite circulation, with the dynamics of each vortex core dominated by the fluid flow pattern of the oppositely charged vortex and by the boundary conditions of the fluid. Although single vortices carry angular momentum, vortex dipoles can be considered as basic topological structures that carry *linear* momentum [1] in stratified or two-dimensional fluids. Vortex dipoles are widespread in classical fluid flows, appearing, for example, in ocean currents [2] and soap films [3], and have been described as the primary vortex structures in two-dimensional chaotic flows [1]. In superfluids, the roles of quantized vortex dipoles appear less well established. Given the prevalence of vortices and antivortices in superfluid turbulence [4–6], the Berezinskii-Kosterlitz-Thouless (BKT) transition [7], and phase transition dynamics [8–11], a quantitative study of vortex dipoles will contribute to a broader and deeper understanding of superfluid phenomena. The realization of vortex dipoles in dilute Bose-Einstein condensates (BECs) is especially significant as BECs provide a clean testing ground for the microscopic physics of superfluid vortices [12–14]. In this Letter we present an experimental and numerical study of the formation, dynamics, and lifetimes of singly and multiply charged vortex dipoles in highly oblate BECs.

Numerical simulations based on the Gross-Pitaevskii equation (GPE) have shown that vortex dipoles are nucleated when a superfluid moves past an impurity faster than a critical velocity, above which vortex shedding induces a drag force [15,16]. Vortex shedding is therefore believed to be a mechanism for the breakdown of superfluidity [17,18]. Experimental studies of periodic stirring of a BEC with a laser beam have measured a critical velocity for the onset of heating and a drag force on

superfluid flow [19,20], and vortex phase singularities have been observed in the wake of a moving laser beam [21,22]. However, a microscopic picture of vortex dipole formation and the ensuing dynamics has not been established experimentally. In the work reported here, single vortex dipoles are deterministically nucleated by causing a highly oblate BEC to move past a repulsive obstacle. We measure a critical velocity for vortex dipole shedding, and find good agreement with numerical simulations and earlier theory [23]. The nucleation process exhibits a high degree of coherence and stability, allowing us to map out the orbital dynamics of a vortex dipole. We find that vortex dipoles can survive for many seconds without self-annihilation. We also provide evidence for the formation of multiply charged vortex dipoles.

The creation of BECs in our lab is described elsewhere [11,24,25]. In the experiments reported here, we begin with a BEC of 2×10^6 ⁸⁷Rb atoms in a highly oblate, axially symmetric harmonic trap created by combining a red-detuned laser light-sheet trapping potential with a magnetic trapping potential. As shown in Figs. 1(a) and 1(b), the BEC has an aspect ratio of $R_r:R_z \sim 11:1$, where $R_r = 52 \mu\text{m}$ is the measured radial Thomas-Fermi radius, and $R_z \sim 5 \mu\text{m}$ is the axial (z) Thomas-Fermi radius. The BECs are additionally penetrated by a focused blue-detuned laser beam that serves as a repulsive obstacle; the beam has a Gaussian $1/e^2$ radius of $10 \mu\text{m}$ and is initially located $20 \mu\text{m}$ to the left of the minimum of the harmonic trap as shown in Fig. 1(c). To nucleate vortices we translate the harmonic potential in the horizontal (x) direction at a constant velocity until the obstacle ends up $14 \mu\text{m}$ to the right of the harmonic trap minimum. At the same time, the height of the obstacle is linearly ramped to zero as shown in Figs. 1(d) and 1(e), allowing us to gently

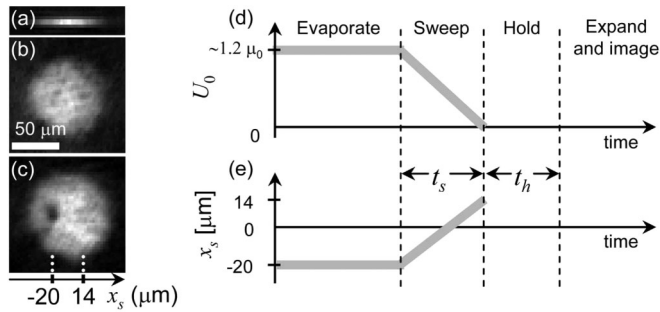


FIG. 1. The BEC initial state and experimental sequence. (a) Side-view phase-contrast image and (b) axial absorption image of a BEC in the highly oblate trap in the absence of the obstacle. Lighter shades indicate higher column densities integrated along the line of sight. Our axial and radial trapping frequencies are measured to be $\omega_z = 2\pi \times (90 \text{ Hz})$ and $\omega_r = 2\pi \times (8 \text{ Hz})$, respectively. (c) BEC initial state with the obstacle located at $x_s = -20 \mu\text{m}$ relative to the BEC center. (d),(e) The maximum repulsive potential energy of the obstacle is $U_0 \approx 1.2\mu_0$ (where $\mu_0 \sim 8\hbar\omega_z$ is the BEC chemical potential) and is held constant during evaporative cooling. It is ramped down linearly as the trap translates; relative to the trap center, the beam moves from position $x_s = -20 \mu\text{m}$ to $x_s = 14 \mu\text{m}$ over a variable sweep time t_s . The BEC is then held in the harmonic trap for a variable time t_h prior to expansion and imaging.

create a vortex dipole that is unaffected by the presence of an obstacle or by heating due to moving the obstacle through the edges of the BEC where the local speed of sound is small. For our conditions, the healing length at the trap center is $\sim 0.3 \mu\text{m}$, which is approximately the size of vortex cores in our trapped BECs. After a subsequent variable hold time t_h we remove the trapping potential and expand the BEC for imaging, causing the vortex cores to expand relative to the condensate radius such that they are optically resolvable. An example axial absorption image is shown in the leftmost inset image of Fig. 2.

In Fig. 2 we plot the average number of vortices observed as a function of the trap translation velocity v_s . In our experimental procedure we find a $\sim 30\%$ likelihood of a single vortex occurring during condensate formation even prior to trap translation; see Ref. [11] for further details. This gives a nonzero probability of observing a single vortex for the lowest translation velocities in Fig. 2 even when flow without drag is expected. The results of zero-temperature and finite-temperature c -field numerical simulations [26] are also shown—for simulation details see Ref. [25]. There is good agreement between simulation and experimental results, and we identify a critical velocity v_c for vortex dipole formation between 170 and 190 $\mu\text{m/s}$ for $N_c = 2 \times 10^6$ atoms and temperature $T = 52 \text{ nK}$. Recently, Crescimanno *et al.* [23] have calculated the critical velocity for vortex dipole formation in a 2D BEC in the Thomas-Fermi regime. By using the nonlinearity and chemical potential of our 3D system in their 2D expression, we estimate a critical velocity of 200 $\mu\text{m/s}$. For our con-

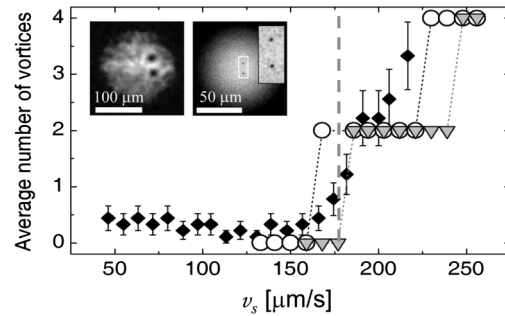


FIG. 2. Average number of vortex cores observed for a range of translation velocities v_s . Experimental data points (black diamonds) are averages of 10 runs each, with error bars showing the standard deviation of the observations. Numerical data for $N_c = 2 \times 10^6$ at a system temperature of $T = 52 \text{ nK}$, corresponding to experimental conditions, are indicated by triangles joined with dotted lines. Fewer atoms and lower temperatures reduce the critical velocity; as an example, open circles show the results of numerical simulations using $N_c = 1.3 \times 10^6$ and $T = 0$. For $v_s \lesssim 170 \mu\text{m/s}$, remnant vortices arising spontaneously during condensate formation (see Ref. [11]) account for the baseline of ~ 0.3 . For $v_s \sim 190 \mu\text{m/s}$, the inset images show a single pair of vortices having formed in the experiment (left) and simulations (right). Because the vortex core diameters are well below our imaging resolution, the BEC is expanded prior to imaging. Similarly, the vortex cores in the unexpanded numerical image are barely visible; a 10- μm -wide inset provides a magnified scale for the core size. Above $v_s \sim 200 \mu\text{m/s}$, multiply-charged vortex dipoles are observed. The critical velocity calculated using the methods of Ref. [23] is indicated by the vertical dashed line.

ditions, the maximum speed of sound at the trap center is calculated to be $c \sim 1700 \mu\text{m/s}$; our measurements show that $v_c \sim 0.1c$, consistent with previous measurements of a critical velocity for the onset of a drag force [20].

In an axisymmetric trap such as ours, a vortex dipole coincides with a meta-stable state of superfluid flow with potentially long lifetimes [27–29]. The vortices exhibit periodic orbital motion, a 2D analogue of the dynamics of a single vortex ring [22,30]. To observe these dynamics we nucleate a single vortex dipole and hold the BEC for variable time t_h prior to expansion and imaging, with results shown in Fig. 3(a). The repeatability and coherence of the vortex nucleation process is clear: in back-to-back images with increasing t_h , the vortex positions and orbital dynamics can be followed and the dipolar nature of the superfluid flow is microscopically determined. These measurements also determine the direction of superfluid circulation about the vortex cores, analogous to the case of single vortices [31]: the image sequence shows counter-clockwise fluid circulation about the vortex core in the upper half of the BEC and clockwise circulation in the lower half. The orbital dynamics were also examined in zero-temperature GPE simulations, as shown in Fig. 3(b) [25], and the experimental and numerical data are in good agreement regarding vortex dipole trajectories, as shown in Fig. 3(c). The lifetime of a single vortex dipole is much

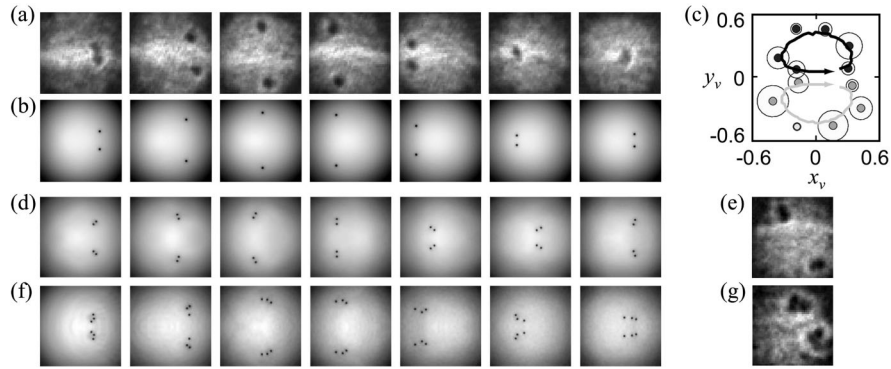


FIG. 3. Sequences of images showing the first orbit of vortex dipole dynamics. (a) Back-to-back expansion images [34] from the experiment with 200 ms of successive hold time between the 180- μm -square images. This sequence was taken using an obstacle height 3.15 times larger than that used for the data of Fig. 2, as this gave the highest degree of repeatability and the least sensitivity to beam displacement. (b) 62- μm -square images from numerical data obtained for conditions similar to the data of sequence (a), but for a temperature of $T = 0$. The orbital period is ~ 1.2 s, and the apparent vortex core size is smaller in the simulations because we show in-trap numerical data. (c) Black and dark gray small circles show average positions x_v and y_v (as fractions of the BEC radius) of each of the two vortices from 5 sequences of experimental data identical to that of sequence (a). The larger circle around each average position point represents the standard deviation of the vortex positions at that specific hold time, and is calculated from the 5 images obtained at that time step. A continuous dipole trajectory from sequence (b) is rescaled to the Thomas-Fermi radius of the expanded experimental images, and superimposed as solid lines on the experimental data; no further adjustments are made for this comparison. (d) Similar to sequence (b), but for a faster translation velocity with which a doubly charged vortex dipole is formed. Images are spaced by 150 ms, and the orbital period is 900 ms. (e) An experimental image of a doubly charged dipole; see text for explanation. (f),(g) Similar to (d) but for a triply charged dipole, 112 ms between images, and an orbital period of 675 ms.

longer than the first orbital period of ~ 1.2 s (see below), although after the first orbit the vortex trajectories become less repeatable from shot-to-shot. However, it is the large-scale flow pattern of the first orbit that is perhaps most indicative of the qualitative connection between 2D superfluid and classical dipolar fluid flows.

For trap translation velocities well above v_c we observe the nucleation of *multiply charged* vortex dipoles both experimentally and numerically, as shown in Figs. 3(d)–3(g). Viewed on a coarse scale the ensuing dynamics are consistent with that of a dipole comprised of a multiply charged vortex and antivortex. On a finer scale, particularly in numerical data, aggregations of singly quantized vortices can be seen near the two loci of vorticity. Figures 3(b), 3(d), and 3(f) show sequences of numerical images that span a single orbital period of the vortex dynamics for singly, doubly, and triply charged dipoles; note that the time intervals for these sequences are different due to differing orbital periods. In experimental images obtained using higher sweep speeds, individual singly charged vortices are often not clearly resolvable for the short hold times of the first dipole orbit. Nevertheless, the data suggest the formation of multiply charged vortex dipoles because (i) the apparent vortex core sizes become larger, (ii) the orbital time period for the dipole structure is shorter, as expected for higher numbers of cores and faster superfluid flow, and (iii) multiple vortex cores are observable for long-enough hold times.

We also note that it might initially be expected that the orbital period of an N -charged dipole should scale inversely with N due to the increase in the velocity field of

a N -charged vortex in a homogeneous BEC. However, simulations and experiments show that this is not the case (see the caption of Fig. 3), and indicate that orbital periods are strongly influenced by the inhomogeneous BEC density. The numerical data of Fig. 3(d) and 3(f) also show small-scale motion of the singly quantized vortices; when finer time scales are examined, it is clear that the individual vortices orbit around each locus of vorticity. These two observations are discussed further in Ref. [25]. Because of the limits of experimental resolution of individual vortices, these small-scale vortex dynamics were not experimentally observable.

It is often assumed that in a finite-temperature environment, vortices of opposite circulation will attract and annihilate each other at close distances. However, our experimental and numerical observations show that vortices may approach each other so closely that they appear to coalesce—see, for example, the sixth image of Fig. 3(a) with $t_h = 1$ s—and yet still move away from each other after the encounter. Similarly, in previous experiments with single vortices in a 2-component BEC, a finite-temperature environment was also observed to have negligible effect on the damping of vortex motion [31]. In Fig. 4 we show measurements of the average number of vortices observed with various hold times after nucleating a vortex dipole, from which we conclude that vortex dipoles may exhibit lifetimes of many seconds, much longer than a single orbital period. With such a strong trap asymmetry, the vortex lines are relatively impervious to bending [32] and tilting [33], and annihilation is suppressed because vortex crossings and reconnections are inhibited.

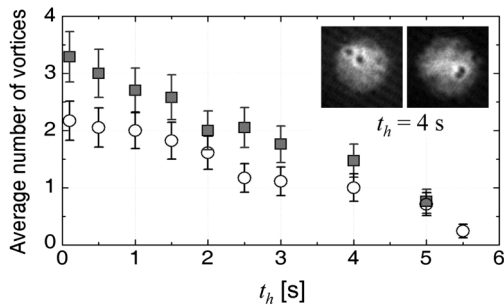


FIG. 4. Number of vortices remaining after dipole nucleation as a function of hold time t_h , averaged over 17 realizations per data point. The circles show conditions for which a singly charged dipole is created, while the squares show data from a faster sweep where four cores (a doubly charged dipole) preferably occur. The error bars represent statistical uncertainty (as in Fig. 2) rather than counting uncertainty; however, for the doubly charged dipole case there is additional uncertainty in counting vortex cores because we do not always resolve 4 well-defined cores at the earlier hold times. The vortex cores can clearly persist for times much longer than the dipole orbital period of ~ 1.2 s for a singly quantized dipole, and ~ 0.8 s for a doubly quantized dipole. Inset figures: experimental images of singly charged dipoles obtained with identical sweeps and held for 4 sec in the trap prior to imaging. The images illustrate the variability of vortex positions after such a long hold time, precluding our ability to track consistent vortex positions beyond one orbital period.

Although vortex shedding is the microscopic mechanism for the breakdown of superfluid flow and the onset of a drag force, the nucleation of a vortex dipole does not imply immediate *heating* since dipoles are coherent structures that are metastable and do not immediately decay into phonons. We estimate that the maximum energy of a vortex dipole in the BEC is $k_B \times 0.45$ nK/atom for our system [19], so that at $T = 52$ nK the temperature would increase by less than 0.5% upon self-annihilation of a single dipole. This temperature change would be difficult to measure, and microscopic observations of vortex dipole formation and dynamics are therefore complementary to heating and drag force observations.

We have demonstrated controlled, coherent nucleation of single vortex dipoles in oblate BECs. The dipole dynamics reveal the topological charges of the vortices and show that the dipole is a long-lived excitation of superfluid flow. Sufficiently rapid translation of the harmonic trap causes vortices with identical charge to aggregate into multiply charged dipolar vortex structures that exhibit orbital dynamics and long lifetimes analogous to singly charged vortex dipoles. This suggests that both dipole structures and macrovortex states are readily accessible in highly oblate and effectively two-dimensional superfluids.

We thank David Roberts for helpful discussions. We acknowledge funding from the U.S. National Science Foundation grant number PHY-0855467, the U.S. Army

Research Office, the New Zealand Foundation for Research, Science, and Technology contract UOOX0801, and the Australian Research Council Centre of Excellence program.

- [1] S.I. Voropayev and Y.D. Afanasyev, *Vortex Structures in a Stratified Fluid* (Chapman and Hall, London, 1994).
- [2] A. Ginzburg and K. Fedorov, Dokl. Akad. Nauk SSSR **274**, 481 (1984).
- [3] Y. Couder and C. Basdevant, J. Fluid Mech. **173**, 225 (1986).
- [4] *Quantized Vortex Dynamics and Superfluid Turbulence*, edited by C.F. Barenghi, R.J. Donnelly, and W.F. Vinen (Springer-Verlag, Berlin, 2001).
- [5] M. Kobayashi and M. Tsubota, Phys. Rev. Lett. **94**, 065302 (2005).
- [6] T.L. Horng, C.H. Hsueh, and S.C. Gou, Phys. Rev. A **77**, 063625 (2008).
- [7] Z. Hadzibabic *et al.*, Nature (London) **441**, 1118 (2006).
- [8] W.H. Zurek, Nature (London) **317**, 505 (1985).
- [9] J.R. Anglin and W.H. Zurek, Phys. Rev. Lett. **83**, 1707 (1999).
- [10] B.V. Svistunov, J. Mosc. Phys. Soc. **1**, 373 (1991).
- [11] C.N. Weiler *et al.*, Nature (London) **455**, 948 (2008).
- [12] A.L. Fetter, Rev. Mod. Phys. **81**, 647 (2009).
- [13] P.G. Kevrekidis *et al.*, Mod. Phys. Lett. B **18**, 1481 (2004).
- [14] *Emergent Nonlinear Phenomena in Bose-Einstein Condensates*, edited by P.G. Kevrekidis, D.J. Frantzeskakis, and R. Carretero-González (Springer-Verlag, Berlin, Heidelberg, 2008).
- [15] T. Frisch, Y. Pomeau, and S. Rica, Phys. Rev. Lett. **69**, 1644 (1992).
- [16] T. Winiecki, J.F. McCann, and C.S. Adams, Phys. Rev. Lett. **82**, 5186 (1999).
- [17] B. Jackson, J.F. McCann, and C.S. Adams, Phys. Rev. Lett. **80**, 3903 (1998).
- [18] T. Winiecki *et al.*, J. Phys. B **33**, 4069 (2000).
- [19] C. Raman *et al.*, Phys. Rev. Lett. **83**, 2502 (1999).
- [20] R. Onofrio *et al.*, Phys. Rev. Lett. **85**, 2228 (2000).
- [21] S. Inouye *et al.*, Phys. Rev. Lett. **87**, 080402 (2001).
- [22] B. Jackson, J.F. McCann, and C.S. Adams, Phys. Rev. A **61**, 013604 (1999).
- [23] M. Crescimanno *et al.*, Phys. Rev. A **62**, 063612 (2000).
- [24] D.R. Scherer *et al.*, Phys. Rev. Lett. **98**, 110402 (2007).
- [25] See supplementary material at <http://link.aps.org/supplemental/10.1103/PhysRevLett.104.160401>.
- [26] P.B. Blakie *et al.*, Adv. Phys. **57**, 363 (2008).
- [27] L.C. Crasovan *et al.*, Phys. Rev. A **68**, 063609 (2003).
- [28] M. Möttönen *et al.*, Phys. Rev. A **71**, 033626 (2005).
- [29] W. Li, M. Haque, and S. Komineas, Phys. Rev. A **77**, 053610 (2008).
- [30] B.P. Anderson *et al.*, Phys. Rev. Lett. **86**, 2926 (2001).
- [31] B.P. Anderson *et al.*, Phys. Rev. Lett. **85**, 2857 (2000).
- [32] V. Bretin *et al.*, Phys. Rev. Lett. **90**, 100403 (2003).
- [33] P.C. Haljan *et al.*, Phys. Rev. Lett. **86**, 2922 (2001).
- [34] The final image of Fig. 3(a) was taken as part of a different sequence, but is included to better illustrate the dipole orbital dynamics.